Minimally Invasive Approach to the Repair of Injured Skeletal Muscle With a Shape-memory Scaffold

Lin Wang[1–4], Lan Cao[1], Janet Shansky[5], Zheng Wang[3,4], David Mooney[1] and Herman Vandenburgh[1,5,6]

[1]School of Engineering and Applied Sciences and Wyss Institute, Harvard University, Cambridge, Massachusetts, USA; [2]Department of Molecular Pharmacology, Physiology, and Biotechnology, Brown University, Providence, Rhode Island, USA; [3]Center for Tissue Engineering and Regenerative Medicine, Union Hospital, Tongji Medical College, Huazhong University of Science and Technology, Wuhan, China; [4]Medical Research Center, Union Hospital, Tongji Medical College, Huazhong University of Science and Technology, Wuhan, China; [5]Myomics, Providence, Rhode Island, USA; [6]Department of Pathology, Brown Medical School–Miriam Hospital, Providence, Rhode Island, USA

Repair of injured skeletal muscle by cell therapies has been limited by poor survival of injected cells. Use of a carrier scaffold delivering cells locally, may enhance *in vivo* cell survival, and promote skeletal muscle regeneration. Biomaterial scaffolds are often implanted into muscle tissue through invasive surgeries, which can result in trauma that delays healing. Minimally invasive approaches to scaffold implantation are thought to minimize these adverse effects. This hypothesis was addressed in the context of a severe mouse skeletal muscle injury model. A degradable, shape-memory alginate scaffold that was highly porous and compressible was delivered by minimally invasive surgical techniques to injured tibialis anterior muscle. The scaffold controlled was quickly rehydrated *in situ* with autologous myoblasts and growth factors (either insulin-like growth factor-1 (IGF-1) alone or IGF-1 with vascular endothelial growth factor (VEGF)). The implanted scaffolds delivering myoblasts and IGF-1 significantly reduced scar formation, enhanced cell engraftment, and improved muscle contractile function. The addition of VEGF to the scaffold further improved functional recovery likely through increased angiogenesis. Thus, the delivery of myoblasts and dual local release of VEGF and IGF-1 from degradable scaffolds implanted through a minimally invasive procedure effectively promoted the functional regeneration of injured skeletal muscle.

Received 13 December 2013; accepted 16 April 2014; advance online publication 3 June 2014. doi:10.1038/mt.2014.78

INTRODUCTION

Musculoskeletal injuries affect millions of patients worldwide each year,[1,2] often resulting in a significant loss of flexibility and strength. When seriously damaged, skeletal muscle has limited ability to restore morphology and function,[3,4] mainly due to formation of excessive scar tissue during the healing process.[5] It would therefore be desirable to find a repair approach that accelerates the process of muscle healing and reduces the formation of scar tissue. Traditional treatments to repair injured skeletal muscle are mainly conservative approaches such as rest, ice, compression, elevation, use of anti-inflammatory drugs, physical therapy, and in some cases, surgery.[6,7] These approaches may be effective in treating mild cases of muscle injuries, but outcomes are often unsatisfactory in treating more severe or chronic skeletal muscle injuries.[8]

Cell therapy may offer an alternative approach as a potential clinical treatment for the repair of severely damaged skeletal muscle. In previous cell therapy studies, cells were either injected directly to the target area requiring repair,[9] or seeded onto biomaterials implanted at the repair site.[10] However, both approaches are limited by rapid loss in viability of the majority of the cells and low integration of cells into host tissues due to a variety of reasons.[11–14] In scaffold-based approaches, biocompatible scaffolds with various three-dimensional structures are often used as a vehicle to deliver cells to the target areas for the purpose of improving cell long-term survival. Transplantation of these scaffolds to the injury sites normally requires surgery. However, theses surgeries themselves often cause unwanted effects affecting the tissue repair process, such as postoperative pain, multiple and large scars, delayed recovery, and a long healing time. Minimally invasive approaches to delivery of scaffolds may minimize these adverse effects of invasive surgery. After transplantation, depending on the materials used for scaffold synthesis, inefficient degradation of scaffolds can be another major hurdle for tissue engineering and regeneration applications.[15] Overly rapid degradation of scaffolds may lead to open space that is then filled by scar tissue, while excessively slow degradation impedes regeneration by potentially stimulating an enhanced immune response and may require invasive surgical removal of scaffolds.[16] Thus, a scaffold that can be delivered by minimally invasive approaches and has proper degradation dynamics may help reduce surgery-derived trauma.

Correspondence: *Herman Vandenburgh, Department of Pathology, Brown Medical School–Miriam Hospital, Providence, Rhode Island 02912, USA. E-mail: Vandenburghlab@gmail.com*

An increasingly important component of diverse cell therapies are growth factors. Several growth factors are known to aid muscle regeneration.[5,17] Insulin-like growth factor-1 (IGF-1) promotes satellite cell proliferation and regulates muscle fiber regeneration following muscle damage.[13,18] Vascular endothelial growth factor (VEGF) stimulates vascularization,[19–21] which is thought to improve the local microenvironment for transplanted cells and enhance cell survival and engraftment efficiency.[22] Dual delivery of IGF-1 and VEGF has been shown to enhance muscle regeneration.[22] However, a major challenge for applying growth factors is their short *in vivo* half-lives. A slow but sustained release at the site of interest is thought to prolong their regeneration-promoting effects, which can be achieved by using a properly bioengineered scaffold as a delivery vehicle.

In this study, we describe a novel, comprehensive, scaffold-based cell therapy strategy for the repair of injured skeletal muscle with a specific aim to minimize surgical requirement for transplantation and postsurgery removal of scaffolds. Our designed shape-memory, highly porous, biodegradable scaffold[23] served as an ideal candidate system for this repair strategy. The shape-memory properties of this scaffold allow for compression of the scaffold so that it can be implanted through a minimally invasive approach, and then rapidly restored its shape after being rehydrated *in vivo* with the solution containing cells and growth factors. Its biodegradability would eliminate the need for further surgical removal of the implant, as the scaffold degradation dynamics match the natural healing process of muscle.[23] Previous *in vitro* experiments demonstrated that its high porosity provided a favorable microenvironment for cell proliferation and for controlled growth factor release.[23] However, it was unknown whether this scaffold could be used *in vivo* through a minimally invasive approach to improve functional regeneration of a damaged muscle. We now show that the targeted delivery of muscle progenitor cells and growth factors (VEGF and IGF-1) using this degradable scaffold, implanted through a minimally invasive technique, markedly promotes regeneration of muscle tissue following severe muscle damage, leading to a nearly complete functional recovery. Thus, with optimization of multiple key steps of scaffold-based treatment, this novel, comprehensive repair strategy can be a powerful method for regeneration of injured skeletal muscle.

RESULTS

Minimally invasive approach to implanting the shape-memory scaffold as a delivery system of cells and growth factors for treating injured muscle

The mouse tibialis anterior (TA) muscle was severely injured by myotoxin injections covering the full length of the muscle followed by femoral artery ligation (**Figure 1a**), which was expected to result in wide-spread scar formation in large area and complete function loss of this muscle. In this animal injury model, the muscle did not spontaneously show complete healing by 5–6 weeks. The following three treatment methods were tested: (i) implantation of cells + IGF-1 + scaffold (cells/IGF-1/scaffold), (ii) implantation of cells + IGF-1 + VEGF + scaffold (cells/IGF-1/VEGF/scaffold), and (iii) injection of suspended cells + IGF-1 without a scaffold (cells/IGF-1(no scaffold)). The scaffold utilized for the treatments was an alginate scaffold comprising 5% oxidized low molecular weight:high molecular weight at a 1:1 ratio,

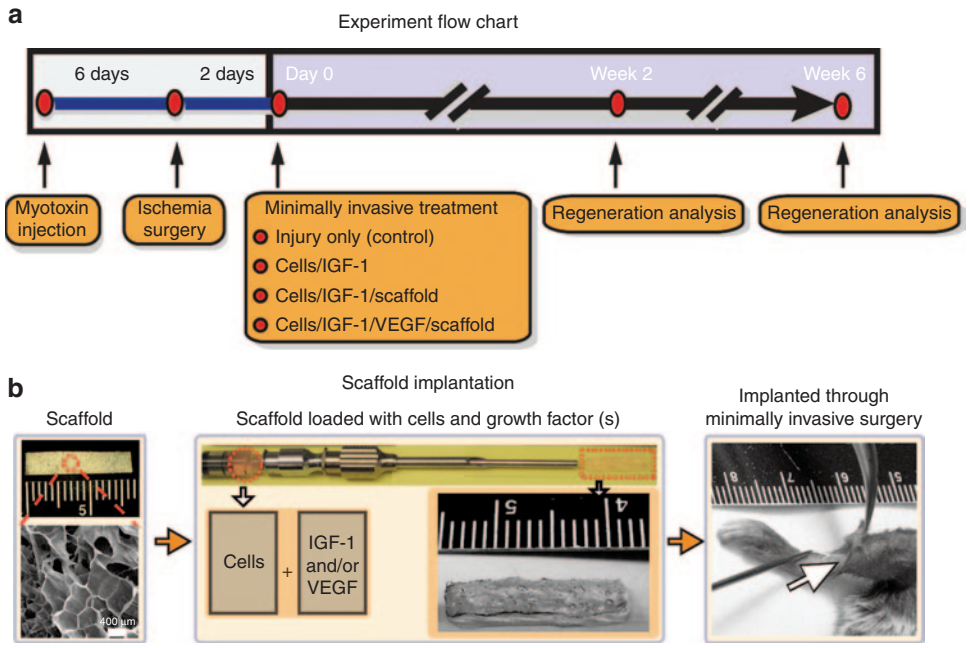

Figure 1 Experimental flow chart and a schematic for the minimally invasive delivery of the scaffold. (**a**) The experimental flow chart. (**b**) Photograph of original macroporous alginate scaffold (16.5 × 2.6 × 0.12 mm) with scanning electron microscopy image (left). Scaffolds had an average pore diameter of 400 µm. Scaffolds were loaded into syringe for delivery via catheter. The middle photograph demonstrates the syringe-needle-catheter device containing a solution of cells and growth factors after the scaffold has been injected; a scaffold (16.5 × 2.6 × 1.1 mm) is also shown following injection and rehydration with cells and growth factors, along with a higher magnification photograph. Scaffolds were implanted subcutaneously along the tibialis anterior via a minimally invasive surgery. Scale bars are shown on images. IGF-1, insulin-like growth factor-1; VEGF, vascular endothelial growth factor.

as described previously.[23] Owing to its unique shape-memory properties (**Supplementary Video S1**),[23] the scaffold was first compressed and implanted along the length of the TA through a 2–3-mm skin incision by being pushed out of a syringe with a plunger (**Figure 1a**; **Supplementary Video S2**). The scaffold was immediately rehydrated *in situ* with a solution of myogenic cells and growth factor(s) as the needle was being withdrawn from the implantation site (**Figure 1b**; **Supplementary Video S2**). The degradation dynamics of the scaffold and drug release profiles of the proteins from it were previously characterized[23–25] (see also Materials and methods).

Scaffolds rehydrated with cells and growth factors significantly reduced muscle fibrosis

At 2 and 6 weeks after the treatments, the TA muscle in the implanted region was analyzed using Masson's trichrome staining to assess scar tissue formation (**Figure 2a–d**). There were no significant differences at week 2 across all the groups, in regards to the amount of fibrotic tissue (**Figure 2e**). However, at week 6, the percent of fibrotic tissue in the cells/IGF-1/scaffold and cells/IGF-1/VEGF/scaffold groups was significantly reduced, by 24 and 44%, respectively, in comparison to the injury-only controls (**Figure 2e**). No significant difference was found between the cells/IGF-1/scaffold and the cells/IGF-1/VEGF/scaffold groups. These results suggest that the inclusion of the scaffold in the treatment can effectively reduce fibrotic tissue within the injured region during muscle regeneration, and VEGF delivery appears to have no effect on fibrotic tissue formation under our experimental conditions. Interestingly, the cells/IGF-1 group had more severe fibrosis than the injured-only control, possibly due to the rapid death of injected muscle cells, which might trigger a local immune response resulting in enhanced fibrosis.

Scaffolds rehydrated with cells and growth factors significantly improved the functional recovery of the injured muscle

To assess muscle functional recovery, the contractile force of the injured TA and muscle wet weight were analyzed during the regeneration process. The maximum contractile force was recorded during tetanic stimulation and normalized to the wet weight of the TA muscle. By 2 weeks after the treatments, the cells/IGF-1/scaffold group showed a slight but significant recovery in contractile force compared to the injury-only controls (**Figure 3a**), indicating that this treatment can lead to functional recovery even at the early stages of regeneration. Remarkably, at week 6, the cells/IGF-1/scaffold and cells/IGF-1/VEGF/scaffold treatments largely restored the contractile force of the damaged muscle, as the force in two groups recovered to 76 and 90% of the unoperated controls, respectively (**Figure 3a**). In contrast, the cell/IGF-1 without the scaffold group showed no significant recovery in contractile force compared to the injury-only controls (**Figure 3a**). These results reveal the important role of the scaffolds in these treatments and suggest that scaffold-based treatments can dramatically improve the long-term functional recovery of the injured muscle. Notably, an additional significant increase in muscle contractile force was observed at week 6 when VEGF was included into the cells/IGF-1/scaffold treatment. This is likely because VEGF-mediated revascularization during TA muscle regeneration (see below) further aids functional recovery.

Moreover, no significant increase in muscle weight was found across all the treatment groups at week 2 (**Figure 3b**). However, the muscle weight of the injury only group was slightly higher ($P < 0.05$) than that of the cells/IGF-1/scaffold group at week 6 after the treatments (**Figure 3b**). Given the reduced fibrotic tissue in the cells/IGF-1/scaffold and cells/IGF-1/VEGF/scaffold groups, this result raised the possibility that the significant functional recovery in these two scaffold-based treatment groups is because their TA muscles contain relative higher fractions of viable and functional muscle tissue.

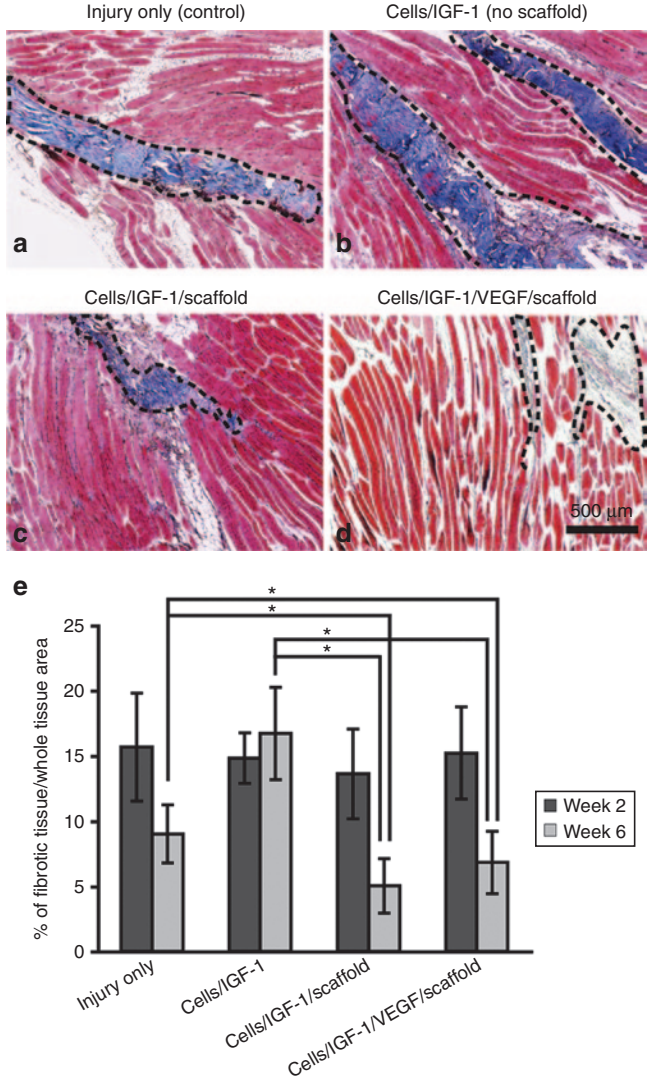

Figure 2 Masson's trichrome staining for fibrotic tissue in longitudinal sections of explanted tibialis anterior muscles at week 6 after the treatments. (**a**) Injury only (controls). Collagen deposition/fibrotic tissue was stained blue (dashed black lines), while the muscle tissue was stained in red. (**b**) Cells/IGF-1 (no scaffold). (c) Cells/IGF-1/scaffold. (**d**) Cells/IGF-1/VEGF/scaffold. (**e**) Quantification of fibrotic tissue area in different treatment groups. The fibrotic tissue area was measured in the Masson's trichrome-stained images 2 and 6 weeks after the treatments, and expressed as the percent of fibrotic tissue area/whole tissue area. The unoperated controls had fibrotic areas of less than 5% (data not shown). Bars represent the mean ± SEM. *$P < 0.05$ ($n = 9–12$). IGF-1, insulin-like growth factor-1; VEGF, vascular endothelial growth factor.

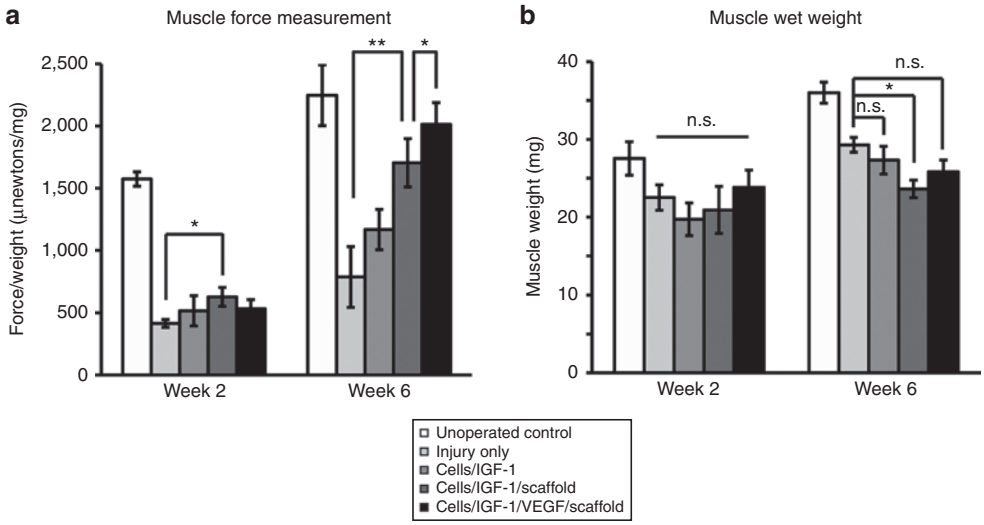

Figure 3 The recovery of muscle force and muscle weight after the treatments. (**a**) Quantification of force of the tibialis anterior (TA) muscles in the different groups at week 2 and week 6 after the treatments. The muscle forces were normalized to the wet weight of the corresponding muscles, and the force/weight ratio was used to indicate recovery of muscle function. Bars represent the mean ± SEM. *$P < 0.05$; **$P < 0.01$ ($n = 5$–8 per treatment group). (**b**) Quantification of TA muscle wet weight in the different groups at week 2 and week 6 after the treatments ($n = 9$–12 per treatment group). Bars represent the mean ± SEM. *$P < 0.05$; n.s., not significant. IGF-1, insulin-like growth factor-1; VEGF, vascular endothelial growth factor.

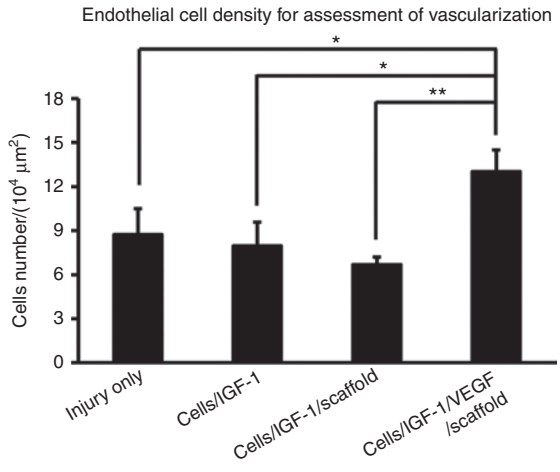

Figure 4 Endothelial cell density in the muscle tissue. At week 6 after the treatments, the average number of vascular endothelial cells (CD31 staining positive, see "Materials and methods" for details) per 10^4 μm^2 tissue area was counted. Bars represent the mean ± SEM. *$P < 0.05$; **$P < 0.01$ ($n = 9$–12). IGF-1, insulin-like growth factor-1; VEGF, vascular endothelial growth factor.

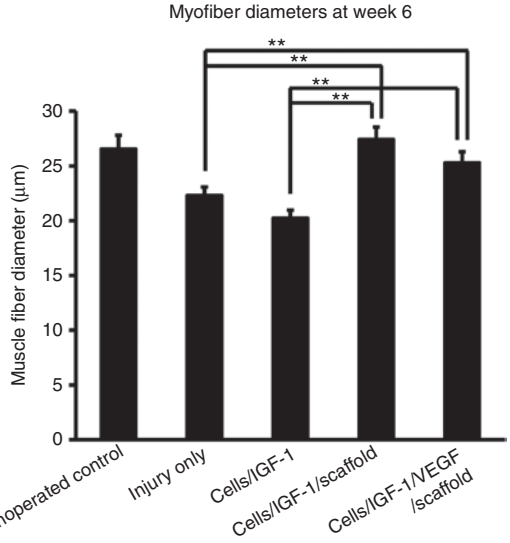

Figure 5 Myofiber diameters at week 6 after the treatments. Muscle fiber cross-sectional areas were measured with ImageJ software. The fiber diameters were calculated from the area measurements. Bars represent the mean ± SEM of each group ($n = 9$–12). **$P < 0.01$. IGF-1, insulin-like growth factor-1; VEGF, vascular endothelial growth factor.

Addition of VEGF to the scaffold-based cell and growth factor treatment improves vascularization in the injured TA muscle

Blood supply is critical for the regeneration of injured muscle tissue.[17,26] To assess revascularization after the injury, an antibody against CD31, a marker for vascular endothelial cells,[25] was used to identify blood vessels in the regenerating TA muscle. The treatment cells/IGF-1/VEGF/scaffold significantly increased the density of vascular endothelial cells compared to the other treatments (**Figure 4**), to a value approximately twice that of the animals receiving the cells/IGF-1/scaffold ($P < 0.01$) at week 6. This result is consistent with VEGF's role in promoting blood vessel formation[19–21,25] and strongly supports the idea that the additional increase observed in muscle functional recovery in the cells/IGF-1/VEGF/scaffold group is due to VEGF-mediated revascularization within the injured area.

Scaffolds rehydrated with cells and growth factors effectively restore the general structural basis of muscle fibers

Muscle fiber diameter, an indicator of an active muscle regenerative process, was quantified for all treatment groups. The mean diameters

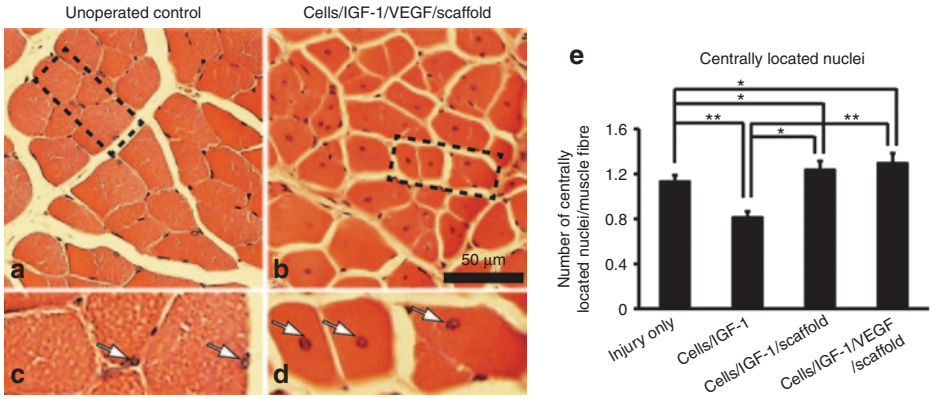

Figure 6 Presence of centrally located cell nuclei in the different groups at week 6 after the treatments. (**a**) Unoperated controls. (**b**) Cells/IGF-1/VEGF/scaffold. (**c** and **d**) Enlarged views of the areas indicated by the dashed lines in (**a**) and (**b**), respectively. Nuclei were indicated by white arrows. (**e**) Quantification of centrally located nuclei in different groups. Bars represent the mean ± SEM. *$P < 0.05$; **$P < 0.01$ ($n = 9$–12). IGF-1, insulin-like growth factor-1; VEGF, vascular endothelial growth factor.

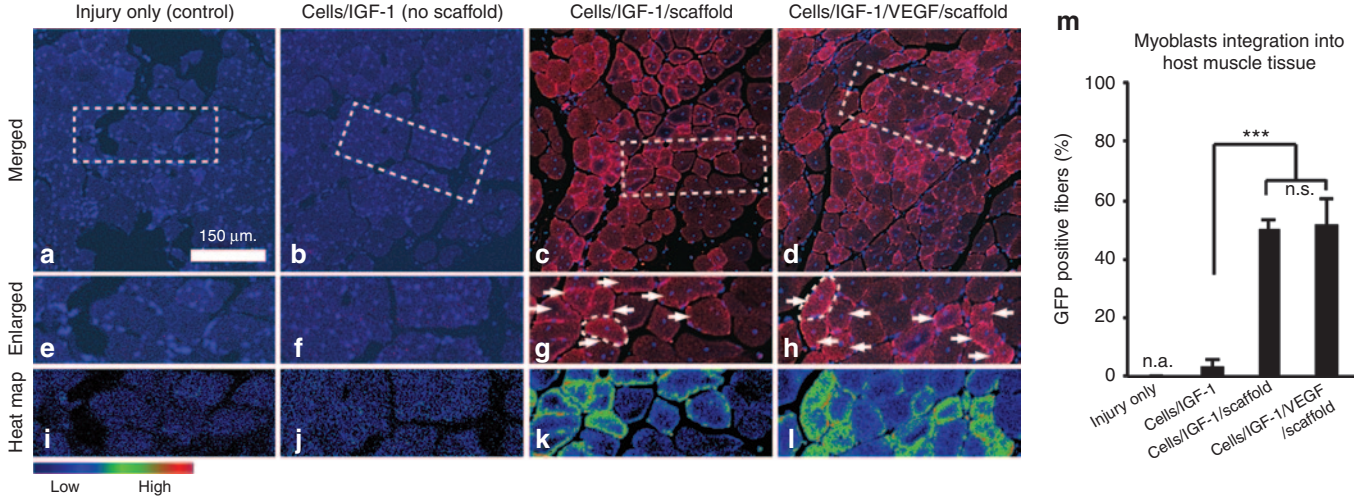

Figure 7 Integration of myoblasts into host muscle tissues. (**a**–**d**) Representative images of green flourescent protein (GFP) staining of tibialis anterior (TA) muscle cross-sections at week 6 after the treatments. GFP staining (pseudored) was merged with the nuclei staining (blue). (**a**) Injury only; (**b**) cells/IGF-1; (**c**) cells/IGF-1/scaffold; (**d**) cells/IGF-1/VEGF/scaffold. (**e**–**h**) Enlarged views of the areas outlined by the white dashed lines in **a**–**d**, respectively; individual myofibers outlined with dashed white lines in (**g**) and (**h**). Positive GFP staining was indicated with arrowheads. (**i**–**l**) The corresponding spectral representation (heat map) of the fluorescence intensity of GFP staining in **e**–**h**. (**m**) Quantification of the percentage of GFP-positive myofibers after the treatments. Bars represent the mean ± SEM. ***$P < 0.001$ (five random fields per slide, three slides per treatment). n.a., not applicable; n.s., not significant. IGF-1, insulin-like growth factor-1; VEGF, vascular endothelial growth factor.

of the muscle fibers in the injured limbs of the animals receiving cells/IGF-1/scaffold with or without VEGF recovered to a level similar to the unoperated controls ($P > 0.1$) (Figure 5), suggesting that these two scaffold-mediated treatments effectively promoted recovery of the muscle structural basis, consistent with the improved muscle function observed for these two groups. In contrast, the treatment cells/IGF-1 had no effect on the muscle fiber diameter, as it was similar to that of the injury-only controls. The average diameters in both of these latter two conditions were significantly smaller than those of the unoperated animals. These results suggest that the scaffolds played a critical role in improving muscle fiber structural recovery when combined with cells and growth factors.

Scaffolds rehydrated with cells and growth factors activate muscle regeneration within injured areas

Centrally located nuclei are an important histological marker for actively regenerating skeletal muscle. To assess the regenerative status of the injured area after the treatments, the density of centrally located nuclei was examined. Both treatments of cells/IGF-1/scaffold with or without VEGF led to a significant increase in the number of centrally located nuclei per muscle fiber, in comparison to the injury-only controls and the cells/IGF-1 group (Figure 6a–e). These results indicate that an active regeneration is ongoing in the animals receiving the scaffold-based treatments. Interestingly, the treatment cells/IGF-1 appeared to inhibit

regeneration, as the density of centrally located nuclei was significantly ($P < 0.01$) lower than that of the injury-only group.

Myoblasts from rehydrated scaffolds are effectively incorporated into local muscle fibers during tissue regeneration

To determine the extent to which the exogenous myoblasts were able to survive, migrate to the injury site from the scaffolds, and fuse with host muscle fibers or form new muscle fibers, myoblasts transduced to express green fluorescent protein (GFP), a visual marker for cell tracking, were used for all the treatments. In the animals receiving the scaffold-based treatments, GFP-positive myofibers were observed by 6 weeks after TA injury with a scattered and uneven distribution throughout the host muscle tissue (**Figure 7c**,**d**,**g**,**h**,**k**,**l**,**m**). GFP staining in the longitudinal sections showed that most of the positively stained muscle fibers were only partially fluorescent along their length, indicating that the delivered cells are likely incorporated into host fibers through fusion, resulting in local GFP expression (**Supplementary Figure S1**). However, a small fraction of new muscle fibers with a large number of GFP nuclei was also observed. The animals receiving the cells/IGF-1 treatment showed very low percentage of GFP-positive myofibers (3%) at week 6 in comparison to ~50% for the cells/IGF-1/scaffold treatment and the cells/IGF-1/VEGF/scaffold treatment (**Figure 7a**,**b**,**e**,**f**,**i**,**j**,**m**). This result indicates that the survival and incorporation of GFP cells in the injured muscle were dramatically reduced without the aid of the scaffold.

DISCUSSION

The challenges facing scaffold-mediated muscle repair exist throughout the muscle regeneration process, including the trauma associated with surgical transplantation of scaffolds, rapid loss of delivered cells, short *in vivo* half-lives of growth factors, and adverse effects due to inefficient degradation of scaffolds. Previous efforts were often orientated toward improving a single aspect of this set. In this study, we propose a comprehensive strategy targeting multiple key aspects of scaffold-mediated treatment, with a focus on a minimally invasive delivery approach. The alginate scaffold used here has the properties of shape memory, high porosity, and preprogrammed degradation dynamics.[23] The shape-memory property permits minimally invasive delivery; high porosity allows high-density cell loading and provides a microenvironment supporting cell survival; degradation dynamics programmed to synchronize with the muscle healing process spares the need for surgical removal and minimizes foreign body inflammatory responses. We show that dealing with multiple regeneration issues significantly promotes muscle functional recovery in a severe skeletal muscle injury model.

Despite tremendous advances in scaffold-based cell therapies, transplantation of scaffolds often requires conventional surgeries that can cause secondary medical injuries, resulting in longer recovery time, and increased risk of infection, bleeding, and scar formation. To minimize surgery-associated injuries, we developed a minimally invasive approach based on the physical properties of these scaffolds.[23] These alginate scaffolds demonstrate hydration-mediated shape memory, allowing for compression before transplantation and delivery through a catheter system. Minimizing the invasiveness required for scaffold placement is expected to decrease the impact on the local physiological conditions and regenerative processes. A different approach to fabricate open-pore, porous scaffolds, also amenable to minimally invasive delivery was recently described.[27] However, those scaffolds were not used to delivery muscle cells or to promote regeneration.

The ultimate goal of muscle injury repair is to improve function. Force measurements reflect the overall muscle functional regeneration. A significant increase in muscle contractile force was observed in this study at week 6 in the animals receiving the scaffold-based treatments. Remarkably, given the fact that this is a severe muscle injury model,[28] the cells/IGF-1/VEGF/scaffold treatment resulted in nearly full functional recovery (90% of the unoperated control). The maximum increase in muscle contraction force was found when VEGF was included in the scaffold treatment, indicating that ischemic muscle function may be improved through VEGF-enhanced revascularization. Supporting this notion, the cells/IGF-1/VEGF/scaffold treatment significantly increased the density of endothelial cells in the injury region. Therefore, VEGF can be an important and valuable component of the scaffold-based treatment repair of muscle injury, consistent with previous studies showing an advantageous role of VEGF in skeletal muscle regeneration.[22,28]

The formation of scar tissue often hinders muscle regenerative processes, resulting in inefficient healing and incomplete function recovery.[5,8] Treatment with the scaffolds delivering cells and growth factor(s) significantly decreased the fibrotic area of the injured TA muscle in this study. This minimization of scar tissue may be due to the continuous myogenic cell migration of the scaffold for integrating into host muscle and the sustained anti-inflammation effects of IGF-1. The active integration of delivered cells with host muscle at the injury site can lead to effective regeneration, which could physically occupy the space that would be otherwise taken by forming scar tissue. This integration requires effective migration of delivered myoblasts from the scaffold. Our alginate scaffold was previously shown to support continuous migration of cells out of the scaffold.[23] Moreover, IGF-1 has anti-necrosis, antiapoptosis, and anti-inflammation effects,[22,29] which would reduce the infiltration of fibroblasts at injured sites. A sustained local release of IGF-1 can prolong these effects, leading to an attenuated inflammatory reaction helping reduce scar formation. In contrast to the differences in fibrotic tissue with scaffold treatment, the total muscle weight remained similar across all the groups at week 6 after the treatments. This suggests that the animals receiving the scaffolds with cells and growth factors may contain more functionally active muscle tissue. This notion was supported by the result showing that the TA muscles in these groups had more significant improvement on force recovery than the other groups. Indeed, the follow-up analyses indicated a more active and effective regeneration in the animals receiving the scaffold-based treatments.

Previous studies suggest that the majority of transplanted cells without scaffolds die quickly after direct intramuscular injection,[12,14] likely because of inflammatory, immune responses.[30,31] Native skeletal muscle extracellular matrix,[32] as well as synthetic matrixes,[33] help protect implanted muscle cells and enhance muscle regeneration. The results presented in this paper support these

observations and expand on earlier work with alginate-based scaffolds for skeletal muscle repair,[22,34] with the development of a minimally invasive treatment strategy using an alginate-based shape-memory material that degrades in a time frame comparable to muscle regeneration.[23]

Cell-cell fusion is critical for myogenesis.[35] During the repair process following muscle injury, myoblasts can fuse with the host or transplanted myoblasts or with the existing muscle fibers at the damaged muscle site, adding their nuclei to the fibers to help promote their regeneration. These fusion events result in an increase in muscle fiber diameter[34] and initially centralized nuclei in the newly fused myoblasts in contrast to peripherally located nuclei in nonregenerating skeletal muscle. Thus, the diameter of muscle fiber and the number of centrally located nuclei are two useful markers for fusion-mediated muscle regeneration process.[36] Given that these two indicators were both significantly improved, in the present study, in the animals receiving the scaffolds-based treatments with cells and growth factor(s), we conclude that cell fusion contributes to the functional and structural repair of injured muscle tissue. This conclusion was further supported by the direct visualization of exogenously delivered GFP-expressing myoblasts being effectively incorporated into host muscle cells. More importantly, this observation is a piece of direct evidence indicating that the exogenous myoblasts are not only capable of migrating out of the scaffolds and surviving for a relatively long time, but remain functionally competent for further differentiation and incorporation with existing muscle.

A challenge facing the translation of this proposed treatment to human is the difficulty of obtaining sufficient amount of patients' autologous myoblasts for delivery within a short timeframe. Identifying the best source and method of preparation of human skeletal muscle stem cells for muscle repair remains a major challenge. For mouse satellite cells, fewer *ex vivo* doublings before implantation improves their *in vivo* regenerative capacity[37] and a similar cell type may exist for human muscle regeneration. An alternative solution would be to implant allogenic myoblasts, which would however require a sustained immunosuppression to avoid the immune rejection of allogenic cells. The risks associated with immunosuppression (cancer and increased infection)[38,39] would limit the treatment to be used in selected patients whose pathological conditions permit a wait. Thus, a future effort directed to achieve fast obtaining/expansion of human autologous myoblasts would be worthwhile.

In summary, our study demonstrates that substantial muscle regeneration can be achieved through a minimally invasive transplantation of an appropriately designed scaffold. Key aspects of the scaffolds include minimally invasive delivery, controlled dual release of growth factors, and improved survival of transplanted cells. Finally, the scaffolds described in the present work degrade *in situ* and thus do not require subsequent surgical removal.

MATERIALS AND METHODS

Skeletal muscle injury model. All animal procedures were performed in compliance with National Institutes of Health and Institutional guidelines. An injury was induced in the TA muscle of 6–7-week-old male C3H/6J mice (Jackson Laboratories, Bar Harbor, ME) by injection of a myotoxin followed by an ischemia surgery several days later. Animals were anesthetized with an intraperitoneal injection of a mixture of ketamine (80 mg/kg) and xylazine (5 mg/kg) prior to all surgical procedures. Fifteen microliters of 10 μg/ml notexin was injected along the long axis of the right TA muscle by a three-point trandermal injection (5 μl injected at each point) using a Hamilton syringe (Hamilton, Reno, NV). Notexin is a phospholipase A2 (PLA2) myotoxin purified from the venom of the Australian tiger snake, *Notechis scutatus*[40] and induces muscle fiber necrosis by binding to the plasma membrane of muscle cells and rupturing it.[41] Six days after notexin injection, animals were anesthetized. The external iliac artery and vein, and the femoral artery and vein, were ligated in the right hind limb. The exposed arterial ends were tied off with 5G nonbioabsorbable sutures; the vessels were cut between the ligation points; the incision was surgically closed. Two days after ischemia was induced, scaffolds were inserted by a minimally invasive technique as described below.

Preparation of biodegradable, shape-memory alginate scaffolds. LF 20/40 alginate was purchased from FMC Biopolymer (Philadelphia, PA). Low molecular weight alginate was generated by gamma irradiation of high molecular weight LF 20/40 alginate (FMC Biopolymer) at a dose of 5.0 Mrad for 4 hours with a cobalt-60 source.[42] Both low molecular weight and high molecular weight alginates were oxidized to 5%,[43] and the resulting oxidized alginate products were further modified with covalently conjugated oligopeptides with RGD peptide (G4RGDSPOH) (Commonwealth Biotechnologies, Richmond, VA) at an average density of 3.4 mmol/l peptide/mol of alginate monomer using carbodiimide chemistry.[44] Scaffolds were formed by standard carbodiimide chemistry as previously described.[45] 5% oxidized low molecular weight and 5% oxidized high molecular weight alginates were combined at a 1:1 weight ratio. The resulting hydrogel was placed in a large volume of distilled water for a minimum of 24 hours, to attain equilibrium swelling and to remove residual unpolymerized chemicals. Alginate scaffolds were then frozen at −20 °C and lyophilized to generate macroporous scaffolds.[46] Scaffolds were cut to desired dimensions (3 × 11 mm) and stored desiccated in a compressed state at room temperature until used.

A number of different formulations for fabricating alginate scaffolds were previously tested.[23] While most scaffolds generated with different formulations had similar shape memory properties, their degradation rates varied greatly. The chosen formulation described above for fabricating the alginate scaffold used in this study was because its degradation rate (complete degradation within 4–6 weeks) matched the natural healing rate of skeletal muscle.[23] 85% of the total scaffold mass was degraded *in vitro* after 28 days; complete degradation was observed after 39 days.[23] Moreover, the drug release property of this scaffold was also previously analyzed.[23] While the half-life of IGF-1 is short (less than 30 minutes *in vivo*), the scaffold as a delivery vehicle prolonged IGF-1 release to 4 days.[23] During the first 3 days, 90% of the IGF-1 was released, which was followed by a sustained slow release from day 3 to 14. By day 14, nearly 100% of IGF-1 was released.

Preparation of myogenic cells. The cells used in this study were clonally derived primary myoblasts that were previously isolated from neonatal mice hindlimb muscle[47] and stably transduced to express GFP using a lentiviral vector system as previously described.[48] Their proliferation on and migration from the scaffold has been previously characterized *in vitro*.[23] Briefly, cells were maintained in skeletal growth medium (1:1 Dulbecco's modified Eagle medium (Gibco, Grand Island NY): fibroblast growth media (Cambrex, Gaithersburg, MD) containing 20% fetal bovine serum (Gibco), 1% ITS-1 (Sigma, St Louis, MO) and 100 U/ml penicillin/100 μg/ml streptomycin) in collagen-coated 10-cm tissue culture dishes in 5% CO_2 at 37 °C. Skeletal growth medium contained 2 μg/ml insulin and 400 ng/ml human fibroblast growth factor. The myoblasts were expanded in culture and harvested by standard tissue culture protocols for rehydrating the scaffold *in vivo*.

Minimally invasive surgical implantation of scaffolds. Scaffold treatment for repair of injured muscle began after notexin injection/ischemic

surgery to TA muscles as described above. The sterile, lyophilized scaffold (13.5 × 2.6 × 1.1 mm) was compressed manually to ~0.12 mm thickness and rolled around an 16-gauge syringe needle to form a tubular shape; it was then inserted into the barrow of a 10-gauge sterile needle (**Figure 1**; **Supplementary Video S2**). A 2-mm incision was made at the ankle site and a "pouch" created over the subcutaneous region of the TA muscle with a dental probe. The skin over the pouch was lifted externally with a forceps. The 10-gauge needle containing the compressed dry alginate scaffold was inserted into the pouch. The scaffold was pushed into the pouch by a 16-gauge needle attached to a syringe containing 50 µl of Dulbecco's modified Eagle medium that contained 0.5×10^6 myoblasts and 3-µg recombinant human IGF-1 (R&D System, Minneapolis, MN), with or without 3-µg VEGF (recombinant human VEGF165, generously provided by Biological Resources Branch of the National Cancer Institute). The scaffold was then immediately rehydrated with this cell and growth factor solution. Controls include the unoperated animals, the animals receiving the injury surgery with no further treatment, and the animals receiving a bolus injection of cells and IGF-1 to the injury site without a scaffold.

Histological and immunocytochemical analyses of TA muscles after treatments. At week 2 and week 6 after the implantation of scaffolds, mice were sacrificed and TA muscles were explanted and processed for histological analyses. TA muscles were harvested from both hind limbs (injured and noninjured), fixed in 4% formaldehyde overnight, washed in saline, embedded in paraffin, and sectioned at 5-µm thickness (Paragon Histology Services, Baltimore, MD). The extent of fibrosis in the TA muscle was analyzed and quantified after Masson's trichrome staining. Briefly, the sections were deparaffinized and processed with a standard Masson's trichrome staining kit (Sigma-Aldrich, St Louis, MO) to distinguish cells from surrounding connective tissues.[48] Cells appeared red/pink; collagen was stained blue; nuclei were stained purple with hematoxylin.[49] Images were taken using a Nikon e600 microscope (×10 or ×20 objectives) equipped with a DP70 camera and analyzed using the software Adobe Photoshop CS. Camera settings were controlled manually and held consistent to produce comparable conditions for image collection. TA muscles from three individual animals were examined for each group. Five areas for each muscle sample were randomly selected for quantification. The area containing the blue signal (collagen) was quantified using the ImageJ software (National Institutes of Health) and expressed as a percentage of the total area.

TA sections were stained with hematoxylin and eosin (H&E) for quantification of fiber diameters and centrally located nuclei. Images were captured with a Nikon e600 microscope (×10 or ×20 objectives) equipped with a DP70 camera and analyzed using the software Adobe Photoshop CS. Three tissue samples from three individual animals were evaluated for each treatment group; six random fields from each sample were selected for analysis using the ImageJ software (National Institutes of Health). The number of centrally located nuclei was counted and normalized to the total number of muscle fibers in each field. The cross-sectional area of each myofiber was measured with the ImageJ software; the fiber diameter was calculated from the area measurement.

CD31 staining was used to identify vascular endothelial cells (EC), using the Tyramide Signal Amplification Biotin System (Perkin Elmer Life Sciences, Boston, MA) to enhance detection. Briefly, deparaffinized sections were rehydrated, blocked for endogenous peroxidase activity and nonspecific interactions, and incubated with an antibody against CD31 (Pharmingen, San Diego, CA) diluted at 1:250 at 4 °C overnight. The sections were then incubated with an anti-rat mouse absorbed biotinylated secondary antibody diluted at 1:200 (Vector Laboratories, Burlingame, CA). A tertiary tyramide signal amplification strepavidin antibody was applied, followed by tyramide signal amplification solution for 7 minutes. The tertiary antibody was then reapplied. Staining was developed using diaminobenzidine + Substrate Chromogen System; DAKO, Carpinteria, CA, and sections were counterstained with hematoxylin. The density of vascular endothelial cell was quantified by normalizing CD31-positive stained areas to the total tissue area.

For identification of GFP-positive myoblasts and myofibers, sections were incubated with an antibody against GFP because high autofluorescence precludes direct visual examination of GFP. Deparaffinized sections were rehydrated, and antigen retrieval was performed by microwaving slides in 10 mmol/l citrate buffer (pH 6.0) for 20 minutes. Slides were cooled, rinsed in PBS, blocked with 5% bovine serum albumin/phosphate-buffered saline for 30 minutes; then incubated with the rabbit polyclonal antibody against GFP (Abcam, Boston, MA) diluted at 1:150 in the blocking buffer overnight at 4 °C in a humidified chamber. Sections were then incubated with AlexaFluor 594-conjugated goat anti-rabbit IgG diluted at 1:200 (Invitrogen, Carlsbad, CA) for 90 minutes in a humidified chamber protected from light at room temperature. Slides were rinsed and cover slipped with the Gold anti-fade reagent with 4',6-diamidino-2-phenylindole (Invitrogen). To quantify the percentage of GFP-positive myofibers, we chose five random fields per slide (three slides per treatment). For each field, the GFP-positive myofibers and total myofibers were counted in ImageJ software. For a specific treatment, the percentage of GFP-positive myofibers from each field was averaged.

Mechanical muscle function measurements. Intact TA muscles were dissected along with their tendons, isolated (n = 5 animals per treatment), mounted vertically between two fine cylindrical parallel steel wire electrodes (1.6 mm in diameter, 21 mm in length), attached by their tendons to microclips connected to a force transducer (FORT 25; WPII, Sarasota, FL), and bathed in a physiological saline solution in a chamber oxygenated with 95% O_2 and 5% CO_2 at 25 °C. Muscle length was adjusted until maximum twitch contractile force was achieved. A wave pulse (100–300 Hz) was initiated from a computer using a custom-written LabView software program and delivered to the stimulation electrodes via a purpose-built power amplifier (QSC USA 1310). A switch on the amplifier permitted stimulation via the wire electrodes.

Contractions were continuously monitored on a LabView virtual chart recorder, and data saved on a computer. Contractions were evoked every 5 minutes. Tetani were usually evoked at 300 Hz, 15–20 V with the constant pulse width and train duration of 2 ms and 1 second, respectively. These stimulation frequencies and voltages were required to generate maximum force but exceed the naturally occurring median firing frequencies of 100–200 Hz in the TA muscle as expected since the muscle is not stimulated through the nerve. After force measurements were completed, the muscles were removed from the bath, blotted, and weighed. Peak tetanic contractile force was determined as the difference between the maximum force during a contraction and the unstimulated baseline level, and specific force calculated by normalization to muscle wet weight.

Statistical analyses. All results are expressed as mean ± standard error of mean. Student's t-tests were used for statistical analysis. Statistical differences were considered significant when $P < 0.05$ and highly significant when $P < 0.01$.

SUPPLEMENTARY MATERIAL

Figure S1. Integration pattern of transplanted myoblasts into host muscle fibers.

Video S1. The shape-memory property of the alginate scaffold.

Video S2. The minimally invasive surgery to deliver the alginate scaffold with cells and growth factors (see also Materials and methods).

ACKNOWLEDGMENTS

We thank Frank Benesch-Lee (Myomics) for assisting in the design and manufacture of the molds for making the scaffolds, Cristina Borselli (Harvard University) for assisting with animal surgeries and experimental techniques, and Geoff Williams (Leduc Bio-imaging facility, Brown University) for imaging assistance. This work was supported by the National Institutes of Health Grants, RO1 DE013349 and R43 AG029705.

REFERENCES

1. McClatchey, KD (2004). Musculoskeletal conditions affect millions. *Arch Pathol Lab Med* **128**: 480.
2. Lubeck, DP (2003). The costs of musculoskeletal disease: health needs assessment and health economics. *Best Pract Res Clin Rheumatol* **17**: 529–539.
3. Järvinen, M (1975). Healing of a crush injury in rat striated muscle. 2. a histological study of the effect of early mobilization and immobilization on the repair processes. *Acta Pathol Microbiol Scand A* **83**: 269–282.
4. Järvinen, M (1976). Healing of a crush injury in rat striated muscle. 4. Effect of early mobilization and immobilization on the tensile properties of gastrocnemius muscle. *Acta Chir Scand* **142**: 47–56.
5. Huard, J, Li, Y and Fu, FH (2002). Muscle injuries and repair: current trends in research. *J Bone Joint Surg Am* **84-A**: 822–832.
6. Järvinen, TA, Järvinen, TL, Kääriäinen, M, Kalimo, H and Järvinen, M (2005). Muscle injuries: biology and treatment. *Am J Sports Med* **33**: 745–764.
7. Järvinen, TA, Järvinen, TL, Kääriäinen, M, Äärimaa, V, Vaittinen, S, Kalimo, H *et al.* (2007). Muscle injuries: optimising recovery. *Best Pract Res Clin Rheumatol* **21**: 317–331.
8. Gates, C and Huard, J (2005). Management of skeletal muscle injuries in military personnel. *Oper Techn Sport Med* **13**: 247–256.
9. Skuk, D and Tremblay, JP (2003). Myoblast transplantation: the current status of a potential therapeutic tool for myopathies. *J Muscle Res Cell Motil* **24**: 285–300.
10. Saxena, AK, Marler, J, Benvenuto, M, Willital, GH and Vacanti, JP (1999). Skeletal muscle tissue engineering using isolated myoblasts on synthetic biodegradable polymers: preliminary studies. *Tissue Eng* **5**: 525–532.
11. Anastasi, S, Giordano, S, Sthandier, O, Gambarotta, G, Maione, R, Comoglio, P *et al.* (1997). A natural hepatocyte growth factor/scatter factor autocrine loop in myoblast cells and the effect of the constitutive Met kinase activation on myogenic differentiation. *J Cell Biol* **137**: 1057–1068.
12. Beauchamp, JR, Morgan, JE, Pagel, CN and Partridge, TA (1999). Dynamics of myoblast transplantation reveal a discrete minority of precursors with stem cell-like properties as the myogenic source. *J Cell Biol* **144**: 1113–1122.
13. Koutsilieris, M, Philippou, A, Maridaki, M and Halapas, A (2007). The role of the insulin-like growth factor 1 (IGF-1) in skeletal muscle physiology. *In Vivo* **21**: 45–54.
14. Qu, Z, Balkir, L, van Deutekom, JC, Robbins, PD, Pruchnic, R and Huard, J (1998). Development of approaches to improve cell survival in myoblast transfer therapy. *J Cell Biol* **142**: 1257–1267.
15. Langer, R and Vacanti, JP (1993). Tissue engineering. *Science* **260**: 920–926.
16. Lanza, RP, Langer, RS and Vacanti, J (2007). *Principles of Tissue Engineering*, Elsevier/ Academic Press: Amsterdam; Boston.
17. Grefte, S, Kuijpers-Jagtman, AM, Toensma, R and Von den Hoff, JW (2007). Skeletal muscle development and regeneration. *Stem Cells Dev* **16**: 857–868.
18. Philippou, A, Halapas, A, Maridaki, M and Koutsilieris, M (2007). Type I insulin-like growth factor receptor signaling in skeletal muscle regeneration and hypertrophy. *J Musculoskelet Neuronal Interact* **7**: 208–218.
19. Coultas, L, Chawengsaksophak, K and Rossant, J (2005). Endothelial cells and VEGF in vascular development. *Nature* **438**: 937–945.
20. Ferrara, N and Kerbel, RS (2005). Angiogenesis as a therapeutic target. *Nature* **438**: 967–974.
21. Ferrara, N, Gerber, HP and LeCouter, J (2003). The biology of VEGF and its receptors. *Nat Med* **9**: 669–676.
22. Borselli, C, Storrie, H, Benesch-Lee, F, Shvartsman, D, Cezar, C, Lichtman, JW *et al.* (2010). Functional muscle regeneration with combined delivery of angiogenesis and myogenesis factors. *Proc Natl Acad Sci USA* **107**: 3287–3292.
23. Wang, L, Shansky, J, Borselli, C, Mooney, D and Vandenburgh, H (2012). Design and fabrication of a biodegradable, covalently crosslinked shape-memory alginate scaffold for cell and growth factor delivery. *Tissue Eng Part A* **18**: 2000–2007.
24. Silva, EA and Mooney, DJ (2007). Spatiotemporal control of vascular endothelial growth factor delivery from injectable hydrogels enhances angiogenesis. *J Thromb Haemost* **5**: 590–598.
25. Silva, EA and Mooney, DJ (2010). Effects of VEGF temporal and spatial presentation on angiogenesis. *Biomaterials* **31**: 1235–1241.
26. Koning, M, Harmsen, MC, van Luyn, MJ and Werker, PM (2009). Current opportunities and challenges in skeletal muscle tissue engineering. *J Tissue Eng Regen Med* **3**: 407–415.
27. Bencherif, SA, Sands, RW, Bhatta, D, Arany, P, Verbeke, CS, Edwards, DA *et al.* (2012). Injectable preformed scaffolds with shape-memory properties. *Proc Natl Acad Sci USA* **109**: 19590–19595.
28. Borselli, C, Cezar, CA, Shvartsman, D, Vandenburgh, HH and Mooney, DJ (2011). The role of multifunctional delivery scaffold in the ability of cultured myoblasts to promote muscle regeneration. *Biomaterials* **32**: 8905–8914.
29. Mourkioti, F and Rosenthal, N (2005). IGF-1, inflammation and stem cells: interactions during muscle regeneration. *Trends Immunol* **26**: 535–542.
30. Smythe, GM, Hodgetts, SI and Grounds, MD (2001). Problems and solutions in myoblast transfer therapy. *J Cell Mol Med* **5**: 33–47.
31. Skuk, D, Caron, N, Goulet, M, Roy, B, Espinosa, F and Tremblay, JP (2002). Dynamics of the early immune cellular reactions after myogenic cell transplantation. *Cell Transplant* **11**: 671–681.
32. Collins, CA, Olsen, I, Zammit, PS, Heslop, L, Petrie, A, Partridge, TA *et al.* (2005). Stem cell function, self-renewal, and behavioral heterogeneity of cells from the adult muscle satellite cell niche. *Cell* **122**: 289–301.
33. Boldrin, L, Elvassore, N, Malerba, A, Flaibani, M, Cimetta, E, Piccoli M *et al.* (2007). Satellite cells delivered by micro-patterned scaffolds: A new strategy for cell transplantation in muscle diseases. *Tissue Eng* **13**: 253–262.
34. Hill, E, Boontheekul, T and Mooney, DJ (2006). Regulating activation of transplanted cells controls tissue regeneration. *Proc Natl Acad Sci U S A* **103**: 2494–2499.
35. Wakelam, MJ (1985). The fusion of myoblasts. *Biochem J* **228**: 1–12.
36. Chargé, SB and Rudnicki, MA (2004). Cellular and molecular regulation of muscle regeneration. *Physiol Rev* **84**: 209–238.
37. Montarras, D, Morgan, J, Collins, C, Relaix, F, Zaffran, S, Cumano, A *et al.* (2005). Direct isolation of satellite cells for skeletal muscle regeneration. *Science* **309**: 2064–2067.
38. Soulillou, JP and Giral, M (2001). Controlling the incidence of infection and malignancy by modifying immunosuppression. *Transplantation* **72**(suppl. 12): S89–S93.
39. Morath, C, Mueller, M, Goldschmidt, H, Schwenger, V, Opelz, G and Zeier, M (2004). Malignancy in renal transplantation. *J Am Soc Nephrol* **15**: 1582–1588.
40. Dixon, RW and Harris, JB (1996). Myotoxic activity of the toxic phospholipase, notexin, from the venom of the Australian tiger snake. *J Neuropathol Exp Neurol* **55**: 1230–1237.
41. Gutiérrez, JM and Ownby, CL (2003). Skeletal muscle degeneration induced by venom phospholipases A2: insights into the mechanisms of local and systemic myotoxicity. *Toxicon* **42**: 915–931.
42. Kong, H, Lee, KY and Mooney, DJ (2002). Decoupling the dependence of rheological/ mechanical properties of hydrogels from solids concentration. *Polymer* **43**: 6239–6246.
43. Boontheekul, T, Kong, HJ and Mooney, DJ (2005). Controlling alginate gel degradation utilizing partial oxidation and bimodal molecular weight distribution. *Biomaterials* **26**: 2455–2465.
44. Rowley, JA, Madlambayan, G and Mooney, DJ (1999). Alginate hydrogels as synthetic extracellular matrix materials. *Biomaterials* **20**: 45–53.
45. Lee KY, Rowley, JA, Eiselt, P, Moy, EM, Bouhadir, KH and Mooney DJ (2000). Controlling mechanical and swelling properties of alginatehydrogels independently of cross-linker type and cross-linking density. *Macromolecules* **33**: 4291–4294.
46. Shapiro, L and Cohen, S (1997). Novel alginate sponges for cell culture and transplantation. *Biomaterials* **18**: 583–590.
47. Vandenburgh, H, Shansky, J, Del Tatto, M and Chromiak, J (1999). Organogenesis of skeletal muscle in tissue culture. *Methods Mol Med* **18**: 217–225.
48. Thorrez, L, Vandenburgh, H, Callewaert, N, Mertens, N, Shansky, J, Wang, L *et al.* (2006). Angiogenesis enhances factor IX delivery and persistence from retrievable human bioengineered muscle implants. *Mol Ther* **14**: 442–451.
49. Liao, H and Zhou, GQ (2009). Development and progress of engineering of skeletal muscle tissue. *Tissue Eng Part B Rev* **15**: 319–331.